DOI 10.24425/aee.2023.147422

Parameter estimation of photovoltaic module relied on golden jackal optimization

THUAN THANH NGUYEN

Faculty of Electrical Engineering Technology
Industrial University of Ho Chi Minh City
No. 12 Nguyen Van Bao, Ward 4, Go Vap District, Ho Chi Minh City, Vietnam
e-mail: nguyenthanhthuan@iuh.edu.vn

(Received: 17.06.2023, revised: 24.08.2023)

Abstract: Due to the nonlinear current-voltage (I-V) relationship of the photovoltaic (PV) module, building a precise mathematical model of the PV module is necessary for evaluating and optimizing the PV systems. This paper proposes a method of building PV parameter estimation models based on golden jackal optimization (GJO). GJO is a recently developed algorithm inspired by the idea of the hunting behavior of golden jackals. The explored and exploited searching strategies of GJO are built based on searching for prey as well as harassing and grabbing prey of golden jackals. The performance of GJO is considered on the commercial KC200GT module under various levels of irradiance and temperature. Its performance is compared to well-known particle swarm optimization (PSO), recent Henry gas solubility optimization (HGSO) and some previous methods. The obtained results show that GJO can estimate unknown PV parameters with high precision. Furthermore, GJO can also provide better efficiency than PSO and HGSO in terms of statistical results over several runs. Thus, GJO can be a reliable algorithm for the PV parameter estimation problem under different environmental conditions.

Key words: golden jackal optimization, henry gas solubility optimization, particle swarm optimization, PV parameter estimation, single diode model

1. Introduction

A high-precise photovoltaic (PV) module model for depicting the PV system characteristic is essential for optimizing its energy. Current-voltage (I-V) and power-voltage (P-V) characters are popular methods to present the non-linear feature of the PV module. I-V and P-V curves are

© 2023. The Author(s). This is an open-access article distributed under the terms of the Creative Commons Attribution-NonCommercial-NoDerivatives License (CC BY-NC-ND 4.0, https://creativecommons.org/licenses/by-nc-nd/4.0/), which permits use, distribution, and reproduction in any medium, provided that the Article is properly cited, the use is non-commercial, and no modifications or adaptations are made.

determined by the mathematical models that consist of a single-diode model (SDM), double-diode model (DDM) and triple-diode model (TDM), where, the SDM is often used to model the PV module. The SDM has unknown parameters that play an important role in building I-V and P-V. The unknown parameters of the PV module can be estimated by the reverse process relying on the experimental data [1]. However, this is a nonlinear problem, which needs efficient solving methods.

There are several methods that have been proposed for the PV parameter estimation problem. They can be classified into categories consisting of deterministic and heuristic methods. In [2], the interval branch and bound method is applied to find the parameters of three types of PV models. In [3], the hybrid approach of numerical and analytical methods is used to find the parameters of PV based on SDM and DDM models. In addition, some works have used the deterministic methods for searching the PV parameters such as [4, 5] and [6]. By using these deterministic methods, a nonlinear characteristic of PV is modeled by using different operation conditions combined with datasheet of manufacturers like current and voltage at a maximum power point, short circuit current and open circuit voltage [7,8]. The common point of this group of methods is that they are described in a complex way, and sometimes the obtained results are affected by the initial values. By using the heuristic methods, the PV parameter estimation problem is considered a type of black-box problem. Thus, it overcomes the disadvantages of the deterministic methods. The main strategy for finding the unknown PV parameters is adjusting the curve to predict the I-V curve, wherein the data points on the predicted I-V curve match with the experiment values. There are several heuristic methods used for the PV parameter estimation problem such as particle swarm optimization (PSO) [9, 10], a genetic algorithm [11], cuckoo search [12], whippy Harris hawks optimization (WHHO) [8], grey wolf optimization (WGO) [13], musical chairs algorithm [14], arithmetic optimization algorithm [15], social spider algorithm (SSA) [16], symmetric chaotic gradient-based optimizer [17], as well as hybrid PSO and WGO [18]. It can be seen that the number of heuristic-based methods is larger than that of deterministic methods. In addition, there are many newly developed algorithms such as Henry gas solubility optimization (HGSO) [19], a coronavirus disease optimization algorithm [20], prairie dog optimization [21], evolutionary mating algorithm [22], etc. and they have also been successfully applied to many problems in electrical engineering such as power quality disturbance [23], optimal power flow [24–26] and distributed generator placement [27]. However, there is no best method for every problem [28]. Some algorithms may produce good results when solving one problem but may give bad results when solving another problem [29]. Thus, the application of new algorithms for the PV parameter estimation problem should be promoted to show the efficiency of the algorithms.

GJO is a recently developed algorithm inspired by the hunting behavior of golden jackals [30]. In nature, they live in groups. In each group, there is usually a pair of male and female leaders. In the process of hunting, golden jackals look for suitable prey, and then they annoy the prey to weaken and attack it. Based on these behaviors, the GJO algorithm was developed that includes an explored search phase based on the process of finding prey and an exploited phase based on the process of harassing and grabbing prey. In [30], the efficiency of GJO was demonstrated, showing several benchmark functions and some engineering problems. However, its performance for the problem of PV parameter estimation is still a query. Therefore, this paper proposes a method for solving the PV parameter estimation problem based on GJO. The contribution of this paper can be summarized as follows:

i. A PV parameter estimation approach relying on GJO is proposed when searching for the parameter set of a PV module model.

ii. The performance of GJO is evaluated on the commercial PV module of KC200GT under different irradiance and temperature levels.

iii. The GJO performance is compared with PSO and HGSO as well as with the previous methods.

The rest of the paper consists of the following parts. The mathematical model of the photovoltaic module and the PV module parameter estimation problem model are shown in Section 2 and Section 3, respectively. The details of the application of golden jackal optimization for estimating the PV parameters are shown in Section 4. The numerical results are demonstrated in Section 5. Finally, the conclusion is presented.

2. Mathematical model of photovoltaic module

There are three types of the equivalent circuit of the PV module consisting of the SDM, DDM and TDM, wherein the SDM is often used to model the PV module. The model of the PV module based on the SDM is presented in Fig. 1.

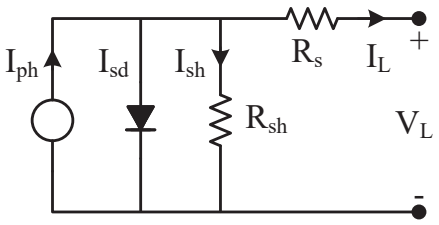

Fig. 1. The equivalent circuit of PV module based on SDM model

The output current of the PV model (I_L) is defined as follows:

$$I_L = I_{ph} - I_{sd} \cdot \left[\exp\left(\frac{q \cdot (V_L + R_s \cdot I_L)}{n_m \cdot k \cdot T} \right) - 1 \right] - \frac{V_L + R_s \cdot I_L}{R_{sh}}, \tag{1}$$

where: I_{ph} is the photocurrent, I_{sd} is the reverse saturation current of the diode, q is the electron charge that is equal to 1.60217646E-19 C, V_L is the output voltage of the cell, R_s is the series resistance, N_c is the number of cells connected in series, n_m is the coefficient that is determined by $n_m = nN_c$, n and N_c are the diode ideality coefficient and the number of serial cells of PV. k is the Boltzmann constant with a value of 1.3806503E-23 J/K. T is the cell temperature in Kelvin. R_{sh} is the shunt resistance.

Equation (1) shows that there are five unknown parameters consisting of I_{ph}, I_{sd}, n, R_s and R_{sh} that need to be estimated from the experimental data of the PV module.

3. Model of the PV module parameter estimation problem

The main objective of the PV module parameter estimation problem is to search for unknown parameters. In order to find these parameters, the problem is converted into an optimization problem. Wherein, the goal is to minimize the difference between the estimated and experimental values. Therefore, the root mean square error (RMSE) of the estimated and experimental values is considered as the objective function of the considered problem that is described as follows:

$$\text{RMSE} = \sqrt{\frac{1}{\text{No}} \sum_{k=1}^{\text{No}} f\left(V_L, I_L, x\right)^2}, \tag{2}$$

where: No is the number of the experimental data, and x is the vector of unknown parameters of the PV module consisting of I_{ph}, I_{sd}, n, R_s, R_{sh}, $f(V_L, I_L, x)$ is determined as follows:

$$f\left(V_L, I_L, x\right) = I_{ph} - I_{sd} \cdot \left[\exp\left(\frac{q \cdot (V_L + R_s \cdot I_L)}{N_c \cdot n \cdot k \cdot T}\right) - 1\right] - \frac{V_L + N_c \cdot R_s \cdot I_L}{R_{sh}} - I_L\,. \tag{3}$$

4. Estimation method of the PV parameters based on golden jackal optimization

Golden jackals live and hunt in pairs, performing the stages of the hunt that include searching and following prey, locking up and irritating prey, and capturing prey. GJO is developed based on the hunting behavior of golden jackals. Details of GJO for the PV module parameter estimation are presented as follows:

Step 1: Generate the initial solution population

In order to solve the parameter estimation problem of the PV module using GJO, each solution is considered as prey. The first and second best solutions are considered as the male and female golden jackals, respectively. At the beginning, the population is created as follows:

$$x_i = \text{rand} \cdot (U - L) + L, \tag{4}$$

where: x_i is the prey i with $i = 1, 2, \ldots, N$, N is the population size, U and L are the upper and lower limit vectors of each solution. Each vector consists of D variables. D is the dimension problem.

Each prey is evaluated by its objective value using (2). Then, the first- and second-best preys are considered as the position of male (x_M) and female (x_{FM}) golden jackals.

Step 2: Update new position

Based on the evading energy of their prey, jackals determine their hunting behavior. The evading energy (E_v) level of the prey is defined as follows:

$$E_v = c_1 \cdot \left(1 - \frac{it}{it_{\max}}\right) \cdot (2 \cdot \text{rand} - 1), \tag{5}$$

where: c_1 is constant with a value of 1.5, it and $it_{\max}$ are the current and maximum number of iterations. From (5), the E_v value will be reduced linearly from c_1 to zero as the number of iterations increases.

In the hunting process, the male golden jackal is the leader, and the female one follows the male jackal. In nature, the prey is not easy to be caught. As the evading energy of prey is high, which is defined by $|E_v| > 1$, the jackals must wait or search for another one. These behaviors are formulated as the exploration or the prey searching strategy of GJO as follows:

$$\begin{cases} x_{i,1} = x_M - E_v \cdot |x_M - c_2 \cdot LF \cdot x_i| \\ x_{i,2} = x_{FM} - E_v \cdot |x_{FM} - c_2 \cdot LF \cdot x_i| \end{cases}, \tag{6}$$

where: $x_{i,1}$ and $x_{i,2}$ are, respectively, the positions of male and female jackals compared to the prey, c_2 is constant with a value of 0.05, and LF is the levy distribution that simulates the movement of the prey to escape the golden jackals.

The evading energy of the prey decreases as it is harassed that is defined by $|E_v| < 1$. Then, a pair of jackals pounce on their prey. These behaviors are formulated as the exploitation, or the prey enclosing and grabbing strategies of GJO as follows:

$$\begin{cases} x_{i,1} = x_M - E_v \cdot |c_1 \cdot LF \cdot x_M - x_i| \\ x_{i,2} = x_{FM} - E_v \cdot |c_1 \cdot LF \cdot x_{FM} - x_i| \end{cases}. \tag{7}$$

Finally, the new position of the prey is updated as follows:

$$x_i = \frac{(x_{i,1} + x_{i,2})}{2}. \tag{8}$$

The new position of the prey is checked and adjusted to its allowed limits as follows:

$$x_{i,j} = \begin{cases} U_j; & \text{if } x_{i,j} > U_j \\ L_j; & \text{if } x_{i,j} < L_j \\ x_{i,j}; & \text{otherwise} \end{cases}, \tag{9}$$

where: $x_{i,j}$ is the variable j with $j = 1, 2, \ldots, D$ of the solution i, U_j and L_j are the upper and lower limits of the variable j.

Then, each prey is evaluated by its objective value using (2). Then, the position of male (x_M) and female (x_{FM}) golden jackals is updated again by comparing their objective value with the objective value of the prey.

Step 3: Stop searching

The process of searching for the optimal solution of GJO for the PV parameter estimation problem is stopped as the current iteration reaches a given maximum value. Then, the position of the male golden jackal is considered as the result. The GJO flowchart for the problem of PV parameter estimation is shown in Fig. 2.

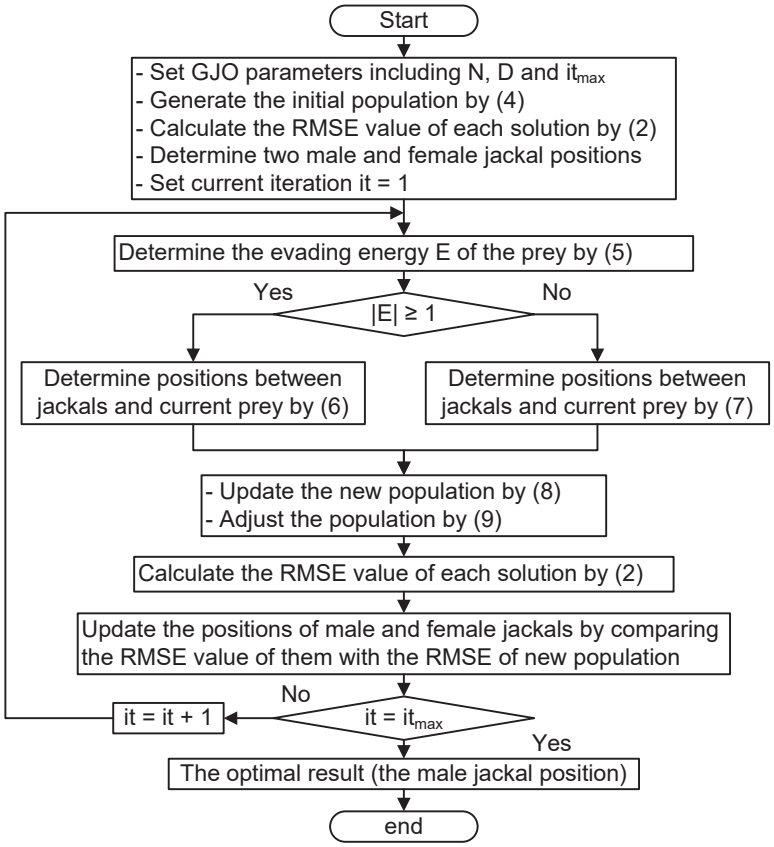

Fig. 2. The flowchart of GJO for the PV parameter estimation problem

5. Results and discussion

To validate the estimation of the parameters of the PV model using GJO, the commercial KC200GT is used to find unknown parameters with different irradiance and temperature levels. The experimental data at irradiance levels of 1 000, 800, 600, 400, and 200 W·m^2 at 25° as well as at temperature levels of 25, 50, and 75° at an irradiance level of 1 000 W·m^2 of this module is directly withdrawn from the I-V curves of its datasheet. The KC200GT datasheet can be taken from [31, 32]. The estimation method of PV model parameters based on GJO is built in Matlab and run on the personal computer. It can be seen that GJO is also based on warm intelligence and individuals tend to follow the leaders. So, in this work, the performance of GJO is compared with the well-known algorithm PSO, which also works based on the aforementioned idea. Moreover, the performance of GJO is also compared with the recent HGSO, which is developed on the grounds of physics-based optimization. For PSO, the learning factor parameters are set to 2 [9, 33]. The maximum number of iterations is chosen to be 2 000. For HGSO, the cluster number is set to 5, and the other constants are selected the same as in [19]. All methods are run 50 times, and the

best solution in these runs is considered as the optimal result. The control variable limits for the PV module are shown in Table 1 [34–36].

Table 1. Parameter Limits of KC200GT

Item	I_{ph}(A)	I_{sd}(μA)	n_m	R_s(Ω)	R_{sh}(Ω)
Lower bound	0	0	1	0.01	100
Upper bound	10	50e-6	60	0.5	1 000

To evaluate the accuracy of the results obtained by GJO, the gained parameters are substituted to the output current of the PV model shown in (1) to determine the calculated current and power at each experimental voltage point. To find the calculated current, a system of nonlinear equations is used [37, 38]. The calculated current (I_{cal}), power (P_{cal}) and the RMSE between the calculated and experimental current, as well as power data, are obtained. Furthermore, the absolute error between the calculated and experimental current (AEI) and the absolute error between the calculated power and experimental power (AEP), which are, respectively, defined as (10) and (11), are also obtained.

$$\text{AEI} = |I_{\text{mea}} - I_{\text{cal}}|\,, \tag{10}$$

$$\text{AEP} = |V_{\text{mea}} \cdot I_{\text{mea}} - V_{\text{mea}} \cdot I_{\text{cal}}|\,. \tag{11}$$

The results of the parameter estimation of the KC200GT module for different irradiation and temperature cases obtained by GJO are presented in Table 2.

Table 2. Estimated parameter of KC200GT by GJO

Irradiation and temperature	I_{ph} (A)	I_{sd} (μA)	n_m	R_s (Ω)	R_{sh} (Ω)
1000 W·m^2, 25°	8.2233	0.0002	52.3491	0.3489	157.6605
800 W·m^2, 25°	6.5444	0.0009	55.8299	0.3349	461.4157
600 W·m^2, 25°	4.9210	0.0042	59.9923	0.2800	426.2278
400 W·m^2, 25°	3.2739	0.0003	53.3692	0.3396	662.0661
200 W·m^2, 25°	1.6452	0.0034	59.8778	0.1754	997.5971
1000 W·m^2, 50°	8.3006	0.0956	58.8863	0.3180	603.8909
1000 W·m^2, 75°	8.4616	1.8264	58.6982	0.3119	285.2745

Based on the parameter estimation results, calculated results for the corresponding irradiations and temperatures are presented in Tables 3–9. Wherein, the number of data points (No) is shown in the first column, the measured voltage V_{mea}), current (I_{mea}) are given in columns 2, 3. The measured power (P_{mea}) that is defined by $V_{\text{mea}} \cdot I_{\text{mea}}$ is given in column 6, while the calculated current (I_{cal}) and power (P_{cal}) values based on the parameters estimated by GJO are given in columns 4 and 7. The absolute error between the calculated and experimental current AEI, and the absolute error between the calculated power and experimental power AEP are shown in column 5 and column 8.

Table 3. Simulated results of GJO for KC200GT at condition of 1 000 W·m^2 and 25°

No	V_{mea}	I_{mea}	I_{cal}	AEI	P_{mea}	P_{cal}	AEP
1	32.8200	0.1559	0.1558	0.0001	5.1166	5.1148	0.0018
2	31.9900	1.6990	1.6954	0.0036	54.3510	54.2364	0.1146
3	30.8300	3.6280	3.6218	0.0062	111.8512	111.6587	0.1925
4	29.9900	4.8180	4.8138	0.0042	144.4918	144.3670	0.1249
5	28.9600	6.0040	5.9980	0.0060	173.8758	173.7028	0.1731
6	27.6100	7.0550	7.0547	0.0003	194.7886	194.7809	0.0077
7	25.9700	7.6970	7.7000	0.0030	199.8911	199.9694	0.0783
8	24.3700	7.9370	7.9405	0.0035	193.4247	193.5104	0.0857
9	21.9700	8.0450	8.0470	0.0020	176.7487	176.7934	0.0447
10	18.7300	8.0840	8.0849	0.0009	151.4133	151.4295	0.0162
11	15.0400	8.1100	8.1098	0.0002	121.9744	121.9719	0.0025
12	11.7400	8.1320	8.1308	0.0012	95.4697	95.4559	0.0138
13	8.8360	8.1520	8.1492	0.0028	72.0311	72.0064	0.0247
14	5.9340	8.1710	8.1676	0.0034	48.4867	48.4664	0.0203
15	3.2960	8.1880	8.1843	0.0037	26.9877	26.9754	0.0123
16	0.0643	8.2100	8.2047	0.0053	0.5279	0.5276	0.0003

Table 4. Simulated results of GJO for KC200GT at condition of 800 W·m^2 and 25°

No	V_{mea}	I_{mea}	I_{cal}	AEI	P_{mea}	P_{cal}	AEP
1	32.4600	0.2478	0.2504	0.0026	8.0436	8.1294	0.0858
2	31.7400	1.4580	1.4683	0.0103	46.2769	46.6049	0.3280
3	31.0500	2.5270	2.5198	0.0072	78.4634	78.2396	0.2237
4	30.2600	3.5810	3.5654	0.0156	108.3611	107.8886	0.4724
5	29.3600	4.5420	4.5305	0.0115	133.3531	133.0142	0.3389
6	28.1200	5.4720	5.4604	0.0116	153.8726	153.5459	0.3268
7	26.8900	5.9920	5.9923	0.0003	161.1249	161.1321	0.0072
8	25.2700	6.2950	6.3144	0.0194	159.0747	159.5660	0.4914
9	23.3200	6.4130	6.4440	0.0310	149.5512	150.2741	0.7230
10	21.4600	6.4480	6.4807	0.0327	138.3741	139.0759	0.7018
11	18.6300	6.4710	6.4975	0.0265	120.5547	121.0491	0.4944
12	15.1300	6.4910	6.5067	0.0157	98.2088	98.4464	0.2376
13	11.5100	6.5100	6.5147	0.0047	74.9301	74.9840	0.0539
14	8.2110	6.5270	6.5218	0.0052	53.5932	53.5508	0.0424
15	4.9150	6.5450	6.5290	0.0160	32.1687	32.0899	0.0788
16	0.2349	6.5700	6.5391	0.0309	1.5433	1.5360	0.0073

Table 5. Simulated results of GJO for KC200GT at condition of 600W·m^2 and 25°

No	V_{mea}	I_{mea}	I_{cal}	AEI	P_{mea}	P_{cal}	AEP
1	32.0600	0.2035	0.1974	0.0061	6.5242	6.3292	0.1950
2	31.2800	1.3690	1.3757	0.0067	42.8223	43.0311	0.2087
3	30.3200	2.5340	2.5455	0.0115	76.8309	77.1782	0.3474
4	29.2700	3.4800	3.4714	0.0086	101.8596	101.6092	0.2504
5	28.0400	4.1750	4.1503	0.0247	117.0670	116.3757	0.6913
6	26.6500	4.5690	4.5491	0.0199	121.7639	121.2343	0.5295
7	25.3500	4.7280	4.7224	0.0056	119.8548	119.7130	0.1418
8	23.6800	4.8060	4.8155	0.0095	113.8061	114.0303	0.2243
9	21.4300	4.8400	4.8566	0.0166	103.7212	104.0766	0.3554
10	18.3300	4.8570	4.8733	0.0163	89.0288	89.3282	0.2994
11	15.0300	4.8710	4.8824	0.0114	73.2111	73.3820	0.1708
12	10.0300	4.8910	4.8943	0.0033	49.0567	49.0894	0.0327
13	4.9520	4.9110	4.9062	0.0048	24.3193	24.2953	0.0239
14	0.1424	4.9300	4.9174	0.0126	0.7020	0.7002	0.0018

Table 6. Simulated results of GJO for KC200GT at condition of 400 W·m^2 and 25°

No	V_{mea}	I_{mea}	I_{cal}	AEI	P_{mea}	P_{cal}	AEP
1	31.6500	0.0069	0.0043	0.0025	0.2168	0.1367	0.0801
2	30.6700	1.1410	1.1389	0.0021	34.9945	34.9307	0.0638
3	29.6900	1.9680	1.9721	0.0041	58.4299	58.5514	0.1215
4	28.1800	2.7200	2.7266	0.0066	76.6496	76.8351	0.1855
5	26.6500	3.0450	3.0533	0.0083	81.1493	81.3692	0.2200
6	25.0300	3.1680	3.1779	0.0099	79.2950	79.5421	0.2470
7	22.8400	3.2170	3.2261	0.0091	73.4763	73.6851	0.2088
8	20.0100	3.2340	3.2405	0.0065	64.7123	64.8430	0.1306
9	15.0700	3.2490	3.2494	0.0004	48.9624	48.9688	0.0064
10	10.0600	3.2620	3.2570	0.0050	32.8157	32.7657	0.0500
11	5.0560	3.2750	3.2646	0.0104	16.5584	16.5057	0.0527
12	0.0505	3.2880	3.2721	0.0159	0.1660	0.1652	0.0008

The results in columns 5 and 8 in the tables show that the absolute error between the experimental data and calculated data is very small at most data points. The I-V and P-V characteristics constructed from the dataset estimated by GJO for the variable irradiance and temperature cases

Table 7. Simulated results of GJO for KC200GT at condition of 200 W·m^2 and 25°

No	V_{mea}	I_{mea}	I_{cal}	AEI	P_{mea}	P_{cal}	AEP
1	30.6900	0.0214	0.0208	0.0007	0.6574	0.6374	0.0199
2	29.5000	0.8035	0.8109	0.0074	23.7033	23.9215	0.2183
3	28.1900	1.2660	1.2555	0.0105	35.6885	35.3927	0.2959
4	26.7300	1.4860	1.4748	0.0112	39.7208	39.4207	0.3001
5	24.9200	1.5790	1.5752	0.0038	39.3487	39.2547	0.0940
6	22.6100	1.6090	1.6122	0.0032	36.3795	36.4529	0.0735
7	20.1000	1.6170	1.6228	0.0058	32.5017	32.6184	0.1167
8	15.0300	1.6250	1.6298	0.0048	24.4238	24.4955	0.0718
9	10.0300	1.6320	1.6349	0.0029	16.3690	16.3976	0.0287
10	5.0280	1.6380	1.6399	0.0019	8.2359	8.2453	0.0094
11	0.0908	1.6450	1.6448	0.0002	0.1494	0.1494	0.0000

Table 8. Simulated results of GJO for KC200GT at condition of 1 000 W·m^2 and 50°

No	V_{mea}	I_{mea}	I_{cal}	AEI	P_{mea}	P_{cal}	AEP
1	29.8900	0.1553	0.1457	0.0096	4.6419	4.3563	0.2856
2	29.2300	1.3610	1.3740	0.0130	39.7820	40.1625	0.3805
3	28.4300	2.7290	2.7443	0.0153	77.5855	78.0214	0.4359
4	27.5500	4.0800	4.0801	0.0001	112.4040	112.4066	0.0026
5	26.7000	5.1850	5.1787	0.0063	138.4395	138.2715	0.1680
6	25.5800	6.3480	6.3178	0.0302	162.3818	161.6094	0.7725
7	23.9700	7.3990	7.3675	0.0315	177.3540	176.5989	0.7551
8	22.0700	7.9450	7.9474	0.0024	175.3462	175.3997	0.0535
9	20.4300	8.1150	8.1431	0.0281	165.7895	166.3641	0.5747
10	18.2300	8.1930	8.2343	0.0413	149.3584	150.1121	0.7537
11	14.9900	8.2320	8.2670	0.0350	123.3977	123.9227	0.5250
12	11.7600	8.2550	8.2762	0.0212	97.0788	97.3279	0.2491
13	8.8590	8.2740	8.2815	0.0075	73.2994	73.3658	0.0664
14	5.8910	8.2940	8.2865	0.0075	48.8600	48.8158	0.0442
15	3.3190	8.3110	8.2908	0.0202	27.5842	27.5171	0.0672
16	0.0878	8.3320	8.2961	0.0359	0.7316	0.7284	0.0032

are shown in Fig. 3 and Fig. 4. The figures show that in all cases, the location of the measured current and power data is located on the calculated curves. This shows that the estimated parameter set obtained by GJO has high accuracy.

Table 9. Simulated results of GJO for KC200GT at condition of 1 000 W·m^2 and 75°

No	V_{mea}	I_{mea}	I_{cal}	AEI	P_{mea}	P_{cal}	AEP
1	26.9000	0.2266	0.2087	0.0179	6.0955	5.6151	0.4804
2	26.2100	1.4640	1.4719	0.0079	38.3714	38.5786	0.2072
3	25.4400	2.7490	2.7672	0.0182	69.9346	70.3970	0.4624
4	24.4900	4.1530	4.1776	0.0246	101.7070	102.3105	0.6035
5	23.5600	5.3300	5.3366	0.0066	125.5748	125.7301	0.1553
6	22.4600	6.4270	6.4096	0.0174	144.3504	143.9585	0.3919
7	21.3300	7.2190	7.1903	0.0287	153.9813	153.3700	0.6112
8	19.9400	7.8050	7.7836	0.0215	155.6317	155.2040	0.4277
9	18.6200	8.1350	8.0884	0.0466	151.4737	150.6056	0.8681
10	17.0300	8.2530	8.2677	0.0147	140.5486	140.7986	0.2500
11	14.9600	8.3320	8.3607	0.0287	124.6467	125.0764	0.4296
12	11.7200	8.3750	8.4050	0.0300	98.1550	98.5068	0.3518
13	8.8830	8.3960	8.4200	0.0240	74.5817	74.7946	0.2130
14	5.9150	8.4170	8.4314	0.0144	49.7866	49.8717	0.0851
15	3.2770	8.4340	8.4408	0.0068	27.6382	27.6605	0.0223
16	0.1113	8.4550	8.4519	0.0031	0.9410	0.9407	0.0003

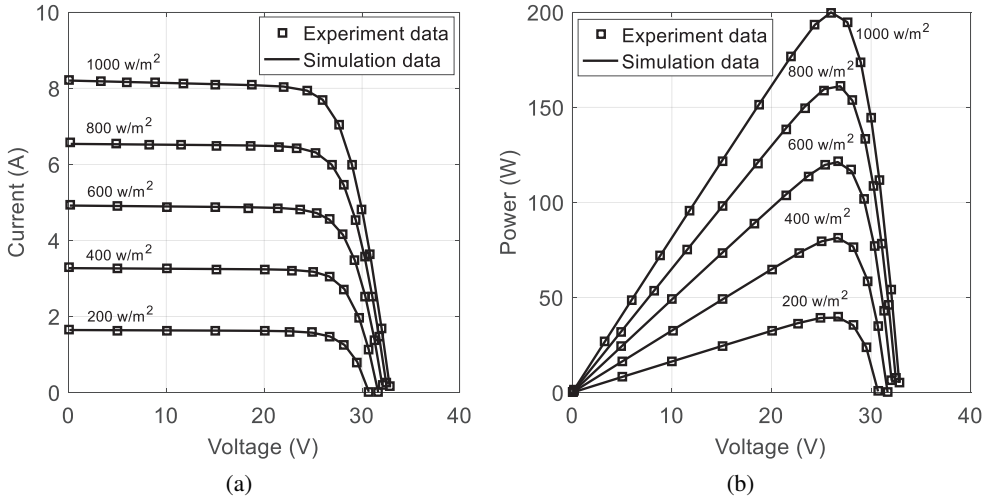

Fig. 3. The experiment and simulation data obtained by GJO for KC200GT module at irradiation levels from 200 to 1 000 W·m^2 at temperature of 25°: I-V curve (a); P-V curve (b)

A comparison of GJO, PSO, and HGSO for all cases of irradiance and temperature in terms of statistical results is shown in Table 10. From the table, the values of all components consisting of the maximum (obj_{max}), minimum (obj_{min}), average (obj_{aver}) objective, and standard deviation (std) in 50 runs of GJO are always lower than those of PSO and HGSO. For the calculated times, the execution time for GJO to search for the optimal solution of the PV module parameter estimation problem is faster than that of HGSO. In comparison with PSO, GJO is slower than that of PSO because the mechanism for updating new solutions of PSO only depends on a velocity expression, which is simpler than the updated mechanisms of GJO. Figure 5 presents the boxplot of GJO, PSO, and HGSO for cases of irradiance of 1 000, 800, 600, 400, and 200 W·m^2 at 25°, and cases of irradiance of 1 000 W·m^2 at 50 and 75°, corresponding to positions from 1 to 7 on the horizontal axis. The figure shows that the fluctuation and concentration tendency of objective values of GJO are much lower than PSO and HGSO. These results confirm the high performance of GJO for the parameter estimation of the PV module.

Table 10. The compared results among GJO, PSO and HGSO at irradiance and temperature levels

Irradiation and temperature	**Method**	**obj_{max}**	**obj_{min}**	**obj_{aver}**	**std**	**Run time (s)**
1 000 W·m^2, 25°	PSO	524.6750	0.5047	35.3192	88.9386	3.3256
	HGSO	2.4274	0.0236	2.2071	0.6669	12.3753
	GJO	2.4252	0.0056	1.1338	1.2041	7.1188
800 W·m^2, 25°	PSO	135.2914	0.7057	21.5304	29.9484	3.4597
	HGSO	1.9334	0.0280	1.8952	0.2695	12.2081
	GJO	1.9333	0.0203	0.6402	0.8962	8.0353
600 W·m^2, 25°	PSO	46.0573	0.4471	9.3466	12.5196	4.3362
	HGSO	1.4020	0.04535	1.3497	0.2579	12.2228
	GJO	1.4017	0.0142	0.4683	0.6477	7.4112
400 W·m^2, 25°	PSO	57.0946	0.5933	9.5941	10.8020	4.4125
	HGSO	0.9550	0.0141	0.9015	0.2124	13.2263
	GJO	0.9544	0.0082	0.3920	0.4640	8.0581
200 W·m^2, 25°	PSO	25.1278	0.1903	5.5655	3.8630	4.4081
	HGSO	0.4351	0.0155	0.4132	0.0891	13.2363
	GJO	0.4350	0.0061	0.2220	0.2153	7.9481
1000 W·m^2, 50°	PSO	7.6889	0.0535	1.7576	1.6476	5.6675
	HGSO	2.6167	0.0299	1.4456	1.2567	15.2491
	GJO	2.6165	0.0271	0.3956	0.9052	7.3281
1000 W·m^2, 75°	PSO	1.1657	0.0308	0.4263	0.3477	4.4641
	HGSO	2.6213	0.0306	0.2117	0.4182	14.9991
	GJO	2.6213	0.0285	0.1392	0.5119	8.0156

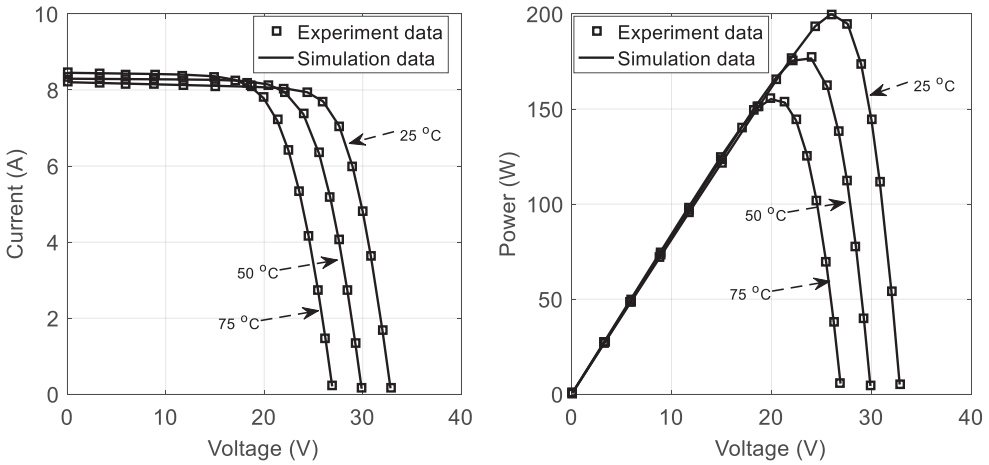

Fig. 4. The experiment and simulation data obtained by GJO for KC200GT module at irradiation level of 1 000 W·m^2 at temperature of 25, 50 and 75°: I-V curve (a); P-V curve (b)

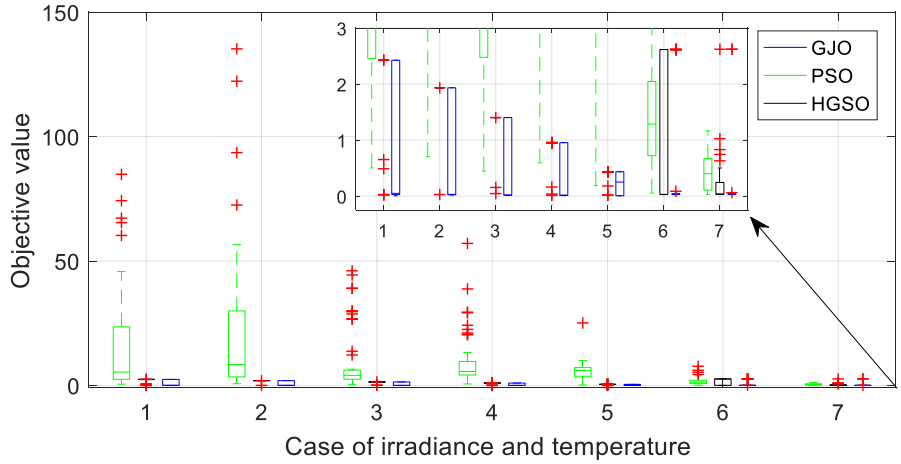

Fig. 5. The boxplot of GJO, PSO and HGSO in 50 runs for irradiation and temperature levels

In comparison with some previous methods, the optimal results obtained by GJO and some other methods for the KC200GT module at 1 000 W·m^2 and 25° are presented in Table 11. The table shows that GJO finds a better RMSE value compared to PSO, HGSO, and the previous methods such as GWO [13], SSA [16], and CWOA [16], while the RMSE gained by GJO is slightly higher than those of SC-GBO [17] and WHHO [8]. This result confirms that the application of GJO for the PV module parameter estimation is reliable.

Table 11. Comparison of GJO and other methods for KC200GT module

Method	I_{ph} (A)	I_{sd} (μA)	n_m	R_s (Ω)	R_{sh} (Ω)	RMSE
GJO	8.2233	0.0002	52.3491	0.3489	157.6605	0.0056
PSO	7.9778	0.0048	60.0000	0.1337	347.5834	0.5047
HGSO	8.2213	0.0023	58.2241	0.3197	201.5652	0.0236
GWO [13]	8.2121	3.2661	75.1518	0.1832	705.1926	0.2100
SSA [16]	8.1445	0.0103	62.4186	0.2196	477.2540	0.0383
CWOA [16]	8.2149	0.0018	57.6126	0.2381	136.0336	0.0283
SC-GBO [17]	8.2168	0.0262	65.4966	0.0048	6.2802	0.0006
WHHO [8]	8.2105	0.0022	57.3210	0.3416	765.3519	0.0015

6. Conclusions

This paper presents a method of estimating the parameters of a photovoltaic module based on GJO. The performance of the proposed GJO for the PV parameter estimation problem is demonstrated via the parameter estimation of the commercial KC200GT module under irradiance levels of 1 000, 800, 600, 400, and 200 W·m^2 at the temperature at 25°, as well as an irradiance level of 1 000 W·m^2, and temperature levels of 25, 50 and 75°. The performance of GJO is compared with PSO and HGSO in terms of statistical results in several independent runs. The numerical results show that the calculated I-V and P-V characteristics of the KC200GT module under different irradiance and temperature levels determined by the proposed GJO method are matched with the extracted dataset. In comparison with PSO and HGSO, GJO reaches better results than PSO and HSGO for most cases of irradiance and temperature, showing lower RMSE values. Furthermore, the results compared with some previous methods also show the reliability of GJO for the considered problem. Therefore, GJO can be a reliable approach for the PV parameter estimation problem under various environmental conditions. In the future, the efficiency of GJO may be applied to determining the parameters of the PV module, taking into account the noise of data.

References

[1] Ibrahim I.A., Hossain M.J., Duck B.C., Nadarajah M., *An improved wind driven optimization algorithm for parameters identification of a triple-diode photovoltaic cell model*, Energy Conversion and Management, vol. 213, 112872 (2020), DOI: 10.1016/j.enconman.2020.112872.

[2] Chenouard R., El-Sehiemy R.A., *An interval branch and bound global optimization algorithm for parameter estimation of three photovoltaic models*, Energy Conversion and Management, vol. 205, 112400 (2020), DOI: 10.1016/j.enconman.2019.112400.

[3] Kumar M., Kumar A., *An efficient parameters extraction technique of photovoltaic models for performance assessment*, Solar Energy, vol. 158, pp. 192–206 (2017), DOI: 10.1016/j.solener.2017.09.046.

[4] Easwarakhanthan T., Bottin J., Bouhouch I., Boutrit C., *Nonlinear Minimization Algorithm for Determining the Solar Cell Parameters with Microcomputers*, International Journal of Solar Energy, vol. 4, no. 1, pp. 1–12 (1986), DOI: 10.1080/01425918608909835.

[5] Changmai P., Nayak S.K., Metya S.K., *Estimation of PV module parameters from the manufacturer's datasheet for MPP estimation*, IET Renewable Power Generation, vol. 14, no. 11, pp. 1988–1996 (2020), DOI: 10.1049/iet-rpg.2019.1377.

[6] AlHajr M.F., El-Naggar K.M., AlRashidi M.R., Al-Othman A.K., *Optimal extraction of solar cell parameters using pattern search*, Renewable Energy, vol. 44, pp. 238–245 (2012), DOI: 10.1016/j.renene.2012.01.082.

[7] Venkateswari R., Rajasekar N., *Review on parameter estimation techniques of solar photovoltaic systems*, International Transactions on Electrical Energy Systems, vol. 31, no. 11, pp. 1–72 (2021), DOI: 10.1002/2050-7038.13113.

[8] Naeijian M., Rahimnejad A., Ebrahimi S.M., Pourmousa N., Gadsden S.A., *Parameter estimation of PV solar cells and modules using Whippy Harris Hawks Optimization Algorithm*, Energy Reports, vol. 7, pp. 4047–4063 (2021), DOI: 10.1016/j.egyr.2021.06.085.

[9] Rezaee Jordehi A., *Enhanced leader particle swarm optimisation (ELPSO): An efficient algorithm for parameter estimation of photovoltaic (PV) cells and modules*, Solar Energy, vol. 159, pp. 78–87 (2018), DOI: 10.1016/j.solener.2017.10.063.

[10] Harrag A., Messalti S., *Three, Five and Seven PV Model Parameters Extraction using PSO*, Energy Procedia, vol. 119, pp. 767–774 (2017), DOI: 10.1016/j.egypro.2017.07.104.

[11] Zagrouba M., Sellami A., Bouaïcha M., Ksouri M., *Identification of PV solar cells and modules parameters using the genetic algorithms: Application to maximum power extraction*, Solar Energy, vol. 84, no. 5, pp. 860–866 (2010), DOI: 10.1016/j.solener.2010.02.012.

[12] Ma J., Ting T.O., Man K.L., Zhang N., Guan S.U., Wong P.W.H., *Parameter estimation of photovoltaic models via cuckoo search*, Journal of Applied Mathematics, vol. 2013, pp. 10–12 (2013), DOI: 10.1155/2013/362619.

[13] Rawat N., Thakur P., Singh A.K., Bhatt A., Sangwan V., Manivannan A., *A new grey wolf optimization-based parameter estimation technique of solar photovoltaic*, Sustainable Energy Technologies and Assessments, vol. 57, 103240 (2023), DOI: 10.1016/j.seta.2023.103240.

[14] Eltamaly A.M., *Musical chairs algorithm for parameters estimation of PV cells*, Solar Energy, vol. 241, pp. 601–620 (2022), DOI: 10.1016/j.solener.2022.06.043.

[15] Mahmoud M.F., Mohamed A.T., Swief R.A., Said L.A., Radwan A.G., *Arithmetic optimization approach for parameters identification of different PV diode models with FOPI-MPPT*, Ain Shams Engineering Journal, vol. 13, no. 3, 101612 (2022), DOI: 10.1016/j.asej.2021.10.007.

[16] Kashefi H., Sadegheih A., Mostafaeipour A., Mohammadpour Omran M., *Parameter identification of solar cells and fuel cell using improved social spider algorithm*, COMPEL – The International Journal for Computation and Mathematics in Electrical and Electronic Engineering, vol. 40, no. 2, pp. 142–172 (2020), DOI: 10.1108/compel-12-2019-0495.

[17] Khelifa M.A., Lekouaghet B., Boukabou A., *Symmetric chaotic gradient-based optimizer algorithm for efficient estimation of PV parameters*, Optik, vol. 259, 168873 (2022), DOI: 10.1016/j.ijleo.2022.168873.

[18] Rezk H., Arfaoui J., Gomaa M.R., *Optimal parameter estimation of solar pv panel based on hybrid particle swarm and grey wolf optimization algorithms*, International Journal of Interactive Multimedia and Artificial Intelligence, vol. 6, no. 6, pp. 145–155 (2021), DOI: 10.9781/ijimai.2020.12.001.

[19] Hashim F.A., Houssein E.H., Mabrouk M.S., Al-Atabany W., Mirjalili S., *Henry gas solubility optimization: A novel physics-based algorithm*, Future Generation Computer Systems, vol. 101, pp. 646–667 (2019), DOI: 10.1016/j.future.2019.07.015.

[20] Khalid A.M., Hamza H.M., Mirjalili S., Hosny K.M., *MOCOVIDOA: a novel multi-objective coronavirus disease optimization algorithm for solving multi-objective optimization problems*, Neural Computing and Applications, vol. 35, no. 23, pp. 17319–17347 (2023), DOI: 10.1007/s00521-023-08587-w.

[21] Ezugwu A.E., Agushaka J.O., Abualigah L., Mirjalili S., Gandomi A.H., *Prairie Dog Optimization Algorithm*, Neural Computing and Applications, vol. 34, no. 22, pp. 20017–20065 (2022), DOI: 10.1007/s00521-022-07530-9.

[22] Sulaiman M.H., Mustaffa Z., Saari M.M., Daniyal H., Mirjalili S., *Evolutionary mating algorithm*, Neural Computing and Applications, vol. 35, no. 1, pp. 487–516 (2023), DOI: 10.1007/s00521-022-07761-w.

[23] Chamchuen S., Siritaratiwat A., Fuangfoo P., Suthisopapan P., Khunkitti P., *Adaptive salp swarm algorithm as optimal feature selection for power quality disturbance classification*, Applied Sciences (Switzerland), vol. 11, no. 12 (2021), DOI: 10.3390/app11125670.

[24] Khunkitti S., Siritaratiwat A., Premrudeepreechacharn S., *A Many-Objective Marine Predators Algorithm for Solving Many-Objective Optimal Power Flow Problem*, Applied Sciences (Switzerland), vol. 12, no. 22 (2022), DOI: 10.3390/app122211829.

[25] Khunkitti S., Siritaratiwat A., Premrudeepreechacharn S., *Multi-objective optimal power flow problems based on slime mould algorithm*, Sustainability (Switzerland), vol. 13, no. 13 (2021), DOI: 10.3390/su13137448.

[26] Al-Kaabi M., Al Hasheme J., Al-Bahrani L., *Improved Differential Evolution Algorithm to solve multi-objective of optimal power flow problem*, Archives of Electrical Engineering, vol. 71, no. 3, pp. 641–657 (2022), DOI: 10.24425/aee.2022.141676.

[27] Branch N., *A new method of decision making in multi-objective optimal placement and sizing of distributed generators in the smart grid*, Archives of Electrical Engineering, vol. 72, no. 1, pp. 253–271 (2023), DOI: 10.24425/aee.2023.143701.

[28] Wolpert D.H., Macready W.G., *No free lunch theorems for optimization*, IEEE Transactions on Evolutionary Computation, vol. 1, no. 1, pp. 67–82 (1997), DOI: 10.1109/4235.585893.

[29] Yang X.-S., *Engineering Optimization: An Introduction with Metaheuristic Applications*, John Wiley & Sons, Inc., Hoboken, New Jersey (2010), DOI: 10.1002/9780470640425.

[30] Chopra N., Mohsin Ansari M., *Golden jackal optimization: A novel nature-inspired optimizer for engineering applications*, Expert Systems with Applications, vol. 198, 116924 (2022), DOI: 10.1016/j.eswa.2022.116924.

[31] Qais M.H., Hasanien H.M., Alghuwainem S., *Parameters extraction of three-diode photovoltaic model using computation and Harris Hawks optimization*, Energy, vol. 195, 117040 (2020), DOI: 10.1016/j.energy.2020.117040.

[32] Qais M.H., Hasanien H.M., Alghuwainem S., Nouh A.S., *Coyote optimization algorithm for parameters extraction of three-diode photovoltaic models of photovoltaic modules*, Energy, vol. 187, 116001 (2019), DOI: 10.1016/j.energy.2019.116001.

[33] Eberhart R., Kennedy J., *A new optimizer using particle swarm theory*, Proceedings of the Sixth International Symposium on Micro Machine and Human Science, Nagoya, Japan, pp. 39–43 (1995), DOI: 10.1109/mhs.1995.494215.

[34] Yu K., Liang J.J., Qu B.Y., Cheng Z., Wang H., *Multiple learning backtracking search algorithm for estimating parameters of photovoltaic models*, Applied Energy, vol. 226, pp. 408–422 (2018), DOI: 10.1016/j.apenergy.2018.06.010.

[35] Zhang Y., Jin Z., Zhao X., Yang Q., *Backtracking search algorithm with Lévy flight for estimating parameters of photovoltaic models*, Energy Conversion and Management, vol. 208, 112615 (2020), DOI: 10.1016/j.enconman.2020.112615.

[36] Derick M., Rani C., Rajesh M., Farrag M.E., Wang Y., Busawon K., *An improved optimization technique for estimation of solar photovoltaic parameters*, Solar Energy, vol. 157, pp. 116–124 (2017), DOI: 10.1016/j.solener.2017.08.006.

[37] Askarzadeh A., Rezazadeh A., *Artificial bee swarm optimization algorithm for parameters identification of solar cell models*, Applied Energy, vol. 102, pp. 943–949 (2013), DOI: 10.1016/j.apenergy.2012.09.052.

[38] Gao X., Cui Y., Hu J., Xu G., Wang Z., Qu J., Wang H., *Parameter extraction of solar cell models using improved shuffled complex evolution algorithm*, Energy Conversion and Management, vol. 157, pp. 460–479 (2018), DOI: 10.1016/j.enconman.2017.12.033.